PERGAMON

Journal of Structural Geology 23 (2001) 865–872

JOURNAL OF STRUCTURAL GEOLOGY

www.elsevier.nl/locate/jstrugeo

Development of crystal morphology during unitaxial growth in a progressively widening vein: I. The numerical model

P.D. Bons*

Earth Processes Simulation Laboratory, Department of Earth Sciences, Monash University, Clayton (Melbourne), VIC 3168, Australia

Received 26 January 1999; accepted 23 November 1999

Abstract

A two-dimensional numerical model for the simulation of the formation of microstructures in crack-seal veins is presented here. The grain aggregate in the vein is described by grain boundary nodes that link short, straight boundary segments. Growth of crystals into a crack takes place by many small incremental movements of nodes. The rate of growth depends on the chosen growth morphology of the vein-forming material. Different growth morphologies can be defined. For every user-defined number of steps, the wall rock is moved a user-defined distance and direction, which simulates the opening of a crack, after which sealing can proceed again. The shape of the crack-surface (e.g. smooth or with ridges) can be set by the user and can be made to match fracture surfaces found in real rocks. The model is capable of reproducing realistic crack-seal textures and can be used to systematically investigate the role of different parameters on the microstructures of veins. First applications of the model are presented in Part II of this paper (this volume).

1. Introduction

Veins are of interest to geologists as each vein represents a stage in the overall geological history of its host rock. The mineral content, shape of the vein and internal microstructure can reveal the geological conditions and operating processes during this stage. Those veins that have very elongate grains form one class of veins that is of particular interest to structural geologists. Such veins may not only preserve information about the average conditions during the vein growth stage, but also the progressive development and changes in conditions during that stage, in particular the maximum incremental stretching or minimum stress direction (Durney and Ramsay, 1973; Ramsay, 1980; Ramsay and Huber, 1983; Passchier and Urai, 1988; Spencer, 1991; Passchier and Trouw, 1996).

This class of veins is generally termed 'fibrous' as individual vein crystals can have rod-shapes with high to very high length/width ratios (Mügge, 1928; Durney and Ramsay, 1973). Fisher and Brantley (1992), and more recently Bons and Jessell (1997), proposed that this class should be subdivided into two: fibrous veins *sensu-stricto* and elongate-blocky veins. Fibrous veins *s.s.* have rod-shaped grains with length/width ratios up to the order of 100:1 and very little variation in individual grain shape (Fig. 1a). Elongate-blocky veins have a larger variation in grain shape and the average grain width increases in the growth direction (Fig. 1b). Many veins that are described in the literature as 'fibrous' would fall into the elongate-blocky category, as are the veins described by Ramsay (1980), which he suggested were formed by the crack-seal mechanism. Crack-seal veins grow by many increments of fracture opening (crack), followed by filling of the fracture by overgrowth of existing vein crystals, exposed to the open fluid-filled fracture (seal). The repeated crack-sealing is usually revealed by vein surface parallel arrays of wall rock inclusions or detached over-growths and fluid inclusions (Ramsay, 1980; Cox and Etheridge, 1983; Ramsay and Huber, 1983; Jessell et al., 1994). Stretched crystals (Durney and Ramsay, 1973) are also sometimes referred to as 'fibres' (Cox and Etheridge, 1983). Stretched crystals are formed by repeated crack-sealing, with subsequent cracks cutting grains at different sites. As a result, very elongate crystals may form (Fig. 1c), which typically have serrated grain boundaries. Cracks cutting stretched crystals probably fill by growth from both crack surfaces, for which Hilgers et al. (2000) propose the term 'bitaxial'. The term 'unitaxial' then refers to cases where growth is only from one side. It is proposed here not to use the term 'fibrous', but only 'stretched crystals' for crystals that grow from repeated crack-sealing at different sites.

Grains in fibrous and elongate-blocky veins often show a

* Now at: Tektonophysik – Institut für Geowissenschaften, Universität Mainz, 55099 Mainz, Germany. Fax: +49-6131-3923863.

E-mail address: bons@mail.uni-mainz.de (P.D. Bons).

0191-8141/01/$ - see front matter
PII: S0191-8141(00)00159-0

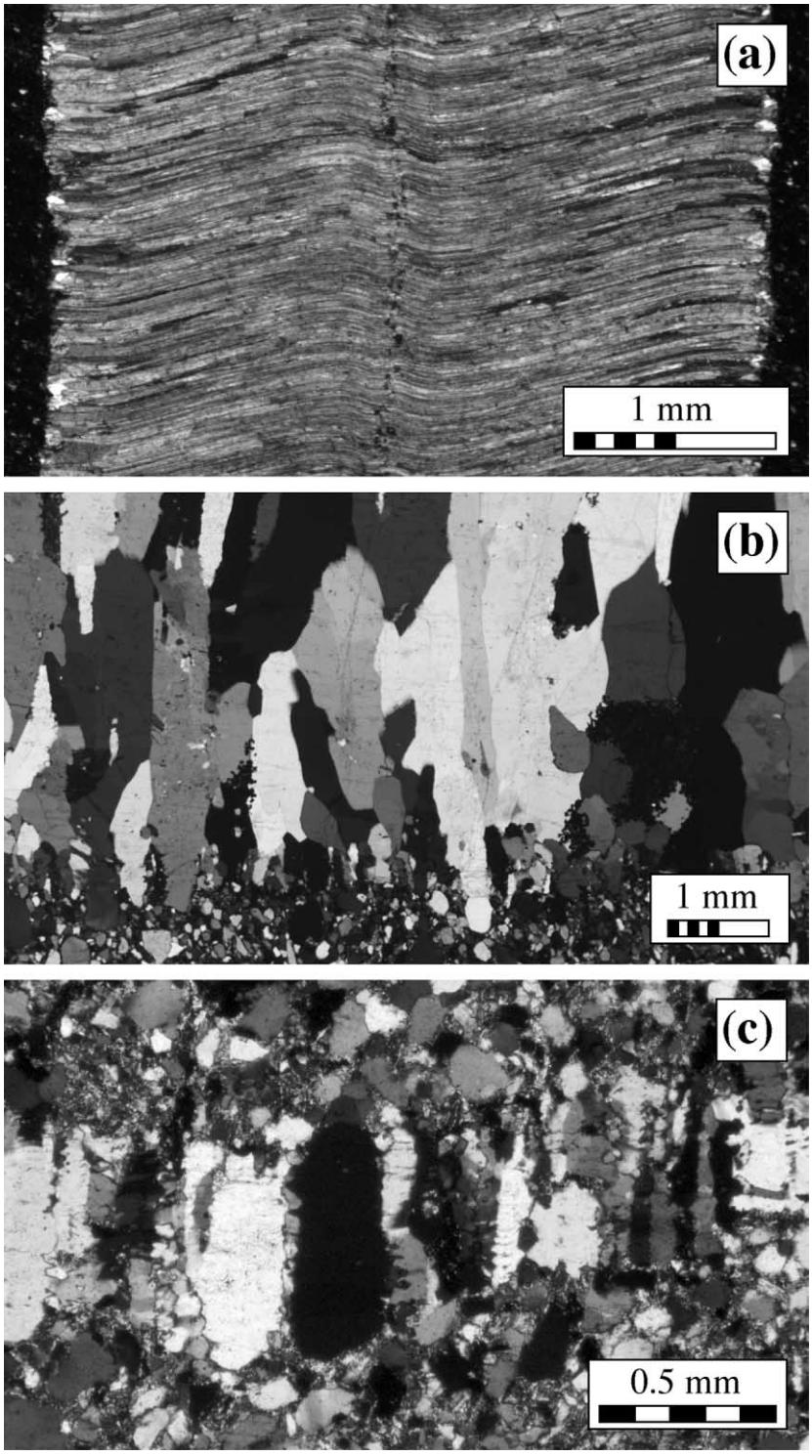

Fig. 1. Photomicrographs of the three vein crystal morphologies that are discussed in this paper. (a) Fibrous crystals in an antitaxial calcite vein in shales at Opaminda Creek, Arkaroola, Northern Flinders Ranges, South Australia. (b) Vein with elongate-blocky quartz crystals that grow towards the top of the image. (c) Small vein with stretched quartz crystals that show typical serrate boundaries. (b) and (c) from folded Palaeozoic turbidites in East Gippsland, Victoria, Australia. All micrographs in cross-polarised light.

curvature. This curvature can be due to post-growth deformation (Williams and Urai, 1989), but in many cases the lattice of such grains is undeformed and other signs of deformation are lacking. In such cases, the curvature can only be attributed to changes in growth direction during vein growth. Initially it was assumed that the growth direction was equal to the opening direction of a vein (Durney and Ramsay, 1973) (Fig. 2a). Hence, the shape of the crystals

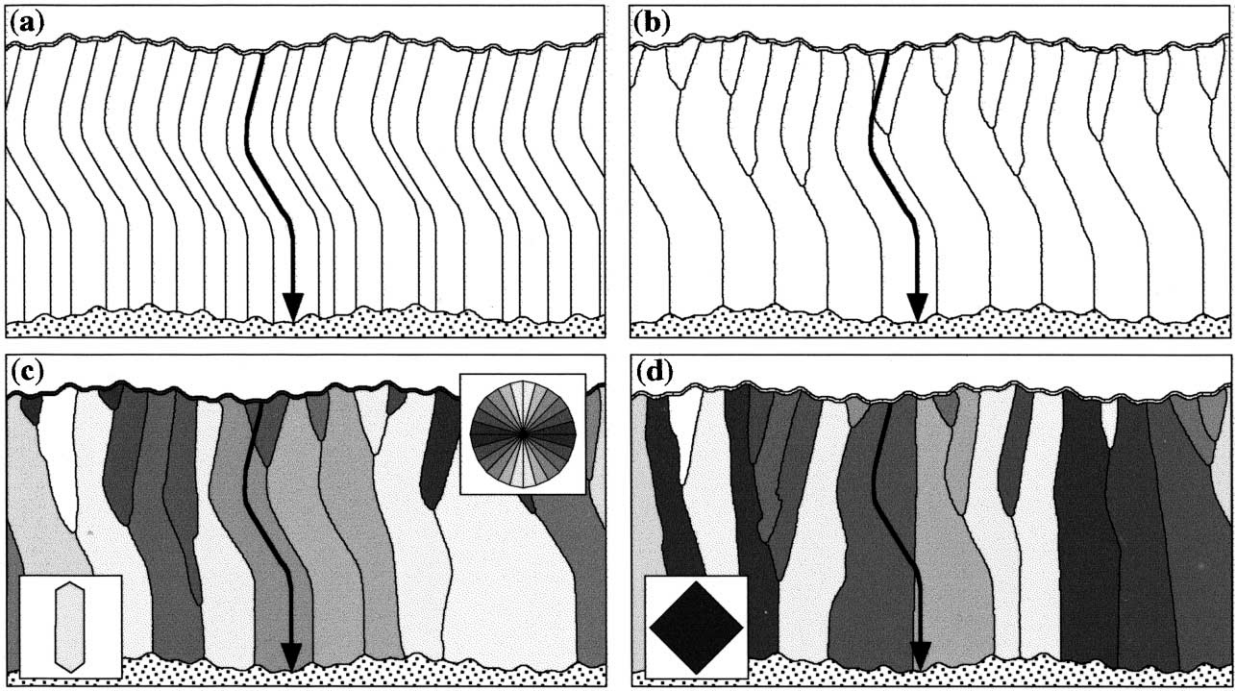

Fig. 2. Models for progressive crystal growth in veins. Crystals grow unitaxially from the top downwards, while the vein opens with a curved trajectory (arrow) in 50 crack-seal events. (a) Perfect tracking of the opening trajectory, according to the model of Durney and Ramsay (1973), resulting in identically shaped fibres. (b–d) Simulations with numerical model presented in this paper: (b) Isotropic growth as in Urai et al. (1991) showing some growth competition due to the roughness of the vein surface. Crystal boundaries get locked onto wall rock ridges, after which tracking becomes perfect. (c) Simulation for a 'mineral' with a prismatic free growth habit (inset), which produces a more varied grain shape and good tracking of only some crystals. *c*-axis orientation of crystals is shown in grey scales, ranging from dark to bright for horizontal to vertical (rose diagram). Light coloured crystals tend to outgrow dark coloured crystals. (d) The same, but for the 'mineral' with a square free growth habit (inset). The difference in growth morphology causes a completely different microstructure.

would exactly track the progressive orientation of maximum stretching or minimum stress during vein growth. Subsequent studies have found that the so-called *tracking capability* is not always perfect (Cox, 1987; Williams and Urai, 1989; Urai et al. 1991). Urai et al. (1991) proposed a model to explain less-than-perfect tracking (Fig. 2b). They proposed that crystals grow outward, i.e. perpendicular to the fracture surface, which, only under particular circumstances, leads to perfect tracking of the opening trajectory. Best tracking is achieved on rough fracture surfaces in narrow fractures.

The numerical model that is presented here builds onto the theory of Urai et al. (1991). It is a computer program that carries out two-dimensional vein growth simulations in accordance with the model of Urai et al. (1991), which allows the user to systematically investigate the effect of different controlling parameters without cumbersome manual work. A major improvement on the work of Urai et al. (1991) is that the current program incorporates the effect of growth anisotropy, which may significantly affect the vein microstructure (Cox and Etheridge, 1983). Minerals that grow into a fluid typically develop faceted crystal faces, according to their mineral-specific crystal morphology. Different growth rates of crystal surfaces lead to growth competition between adjacent grains. This causes grain boundaries to not always extend perpendicular to the local surface. It can also lead to the development of a crystallographic preferred orientation in veins, as some lattice orientations are more favourable for growth and grains with these lattice orientations ('winner grains') outgrow unfavourably oriented grains ('loser grains'). It is clear that growth competition leads to a variable grain shape, an important distinguishing feature between fibrous and elongate-blocky veins (Fig. 2).

2. Description of the numerical routine

A vein in the model consists of a horizontal row of grains. The model is horizontally wrapping around: the grain overlapping with the left end of the row 're-appears' again on the right end (Fig. 3a). Grains are defined by nodes (Fig. 3b), which link short straight grain boundary segments. Growth of grains into the open fracture is simulated by movement of these nodes in many small increments. Growth is unitaxial, with only downwards growth of the crystals from the upper surface of the crack. Node positions are recorded as floating point *X*- and *Y*-coordinates, allowing for arbitrary small growth increments. Grains are seeded on the upper surface of a horizontal fracture. Opening of the fracture is simulated by downward movement of the lower fracture or wall rock surface, relative to the grains that have already grown. The

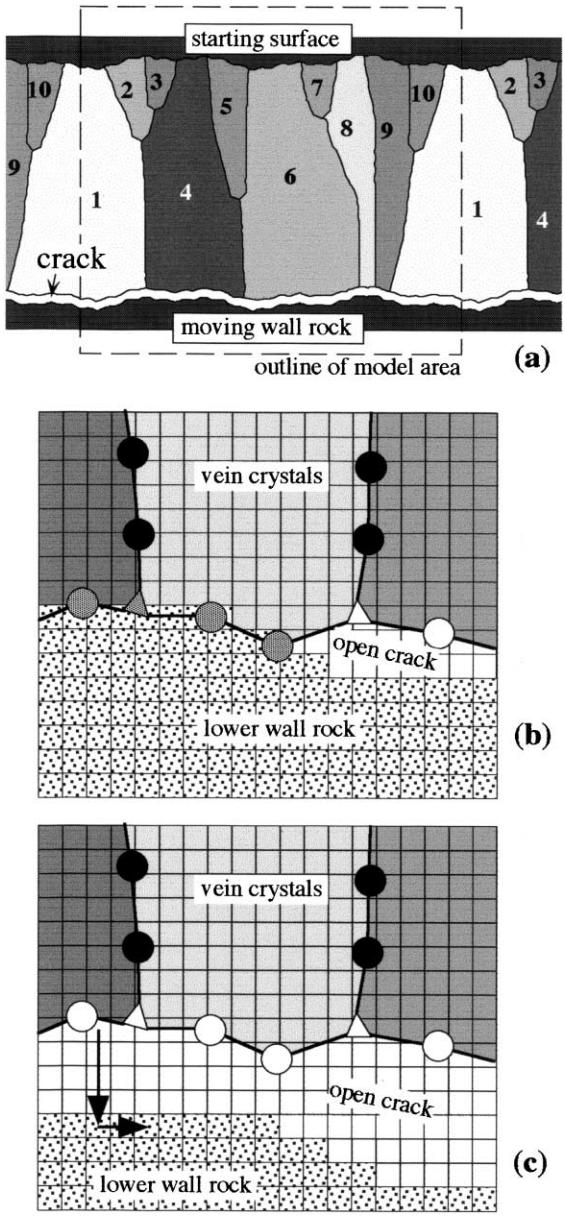

Fig. 3. Basic description of the numerical model. (a) The modelled area (dashed outline) is repeated on both sides. In the example there are 10 grains, with grain 1 occurring both on the left and the right sides of the modelled area. Grains are seeded on a surface at the top, and grow downwards in the space provided by the stepwise moving lower wall rock surface. (b) Detail of the partially sealed crack. Crystals (grey) are bound by nodes that link straight crystal boundary segments. Triangles are triple junctions which link three crystal boundary segments, while circles are nodes that link only two segments. Black nodes are passive and cannot move, while white nodes face the open crack space and are incrementally moved to represent growth of the crystals. Grey nodes lie on bit-map coordinates (dotted area in the square grid) that represent the lower wall rock and are temporarily locked, until the crack opens again. (c) Opening of the crack is performed by changing bit map flags from 'wall rock' (dotted) to 'vein' (white), according to the user-defined opening distance, in this case 4 pixels down and 2 pixels to the right. Temporarily locked nodes are released again for renewed growth.

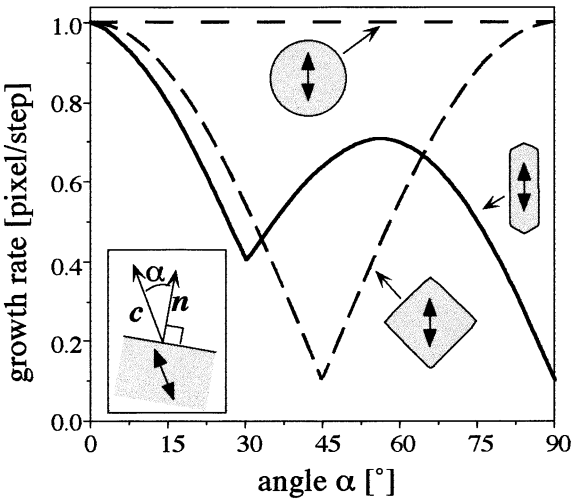

Fig. 4. Growth rate functions (rate versus α) for the 'isotropic' (circle-shaped), 'square' and 'prismatic mineral'. Double arrows represent c-axis orientations. Inset shows the definition of the angle α, which is the angle between the c-axis (c) and the normal to the crystal surface (n). All growth rates are normalised to one pixel per time step for the maximum growth rate, so actual growth rates are between zero and one pixel per time step.

model thus simulates vein growth in one half of an antitaxial vein (Ramsay and Huber, 1983), where unitaxial growth occurs from the vein outwards at the vein–wall rock interface.

There are three modes of activity for nodes (Fig. 3b and c):

1. Passive nodes that are not on the growth surface of the grains. These nodes never move.
2. Active nodes that lie on the growth surface of grains where it is in contact with open fracture space. These nodes are moved to simulate growth of crystals. All active nodes are moved once every time step.
3. Locked nodes. These nodes are on the growth surface of grains, but also lie on the wall rock surface and can therefore not move further until the next fracture opening event.

The fracture–wall rock surface is defined by a list of integer X- and Y-coordinates from left to right. Any wall rock geometry can be created with the only restriction being that there can only be one Y-coordinate for each X-coordinate. During run time of the program, this is translated to a bitmap that corresponds to the square screen pixels (Fig. 3b). All pixels above the wall rock are labelled 'vein', while all on or below the wall rock surface are labelled 'wall rock'. As soon as a node moves onto a wall rock pixel, the node reverts from active mode to locked. The wall rock surface is moved every user-defined number of time steps over a user-defined whole number of pixels down and to the left or right (Fig. 3c). Different stages in crack opening frequency, distance and direction can be set by the user at the start of the program.

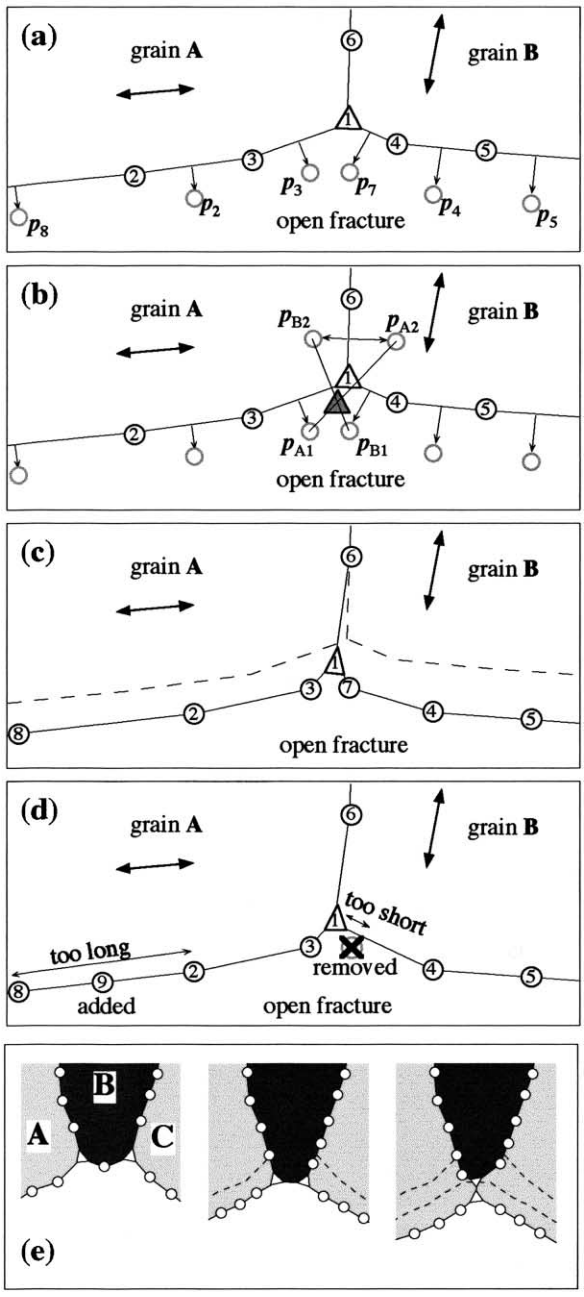

Fig. 5. Explanation of the routines to move nodes to simulate growth. See text for full discussion. (a) First the new positions ($\boldsymbol{p}$) are calculated of nodes that join two boundary segments. A new node has to be created for the segment to the right of the triple junction (node 7). (b) Next, the new positions of triple junction nodes are calculated. (c) The nodes are actually moved after all new positions have been calculated. (d) After one movement step, all segments are checked for their length. If a segment is too long (between nodes 8 and 2), a new node is inserted halfway (node 9). If, on the other hand, the distance between two nodes on either side of a node is too short (between nodes 1 and 4), that node is removed (node 7). This way, a roughly constant segment length is achieved. (e) When two triple junction nodes converge, a neighbour-switch is carried out: in the example, grains A and C become neighbours and grain B looses contact with the growth surface.

2.1. Growth morphology

Each grain has a *c*-axis orientation (0–180°) as an attribute. The growth rate is a function of the angle (α) between the *c*-axis and the normal to a surface segment of a grain. This morphology function can be set by the user to create any desired growth morphology. Three morphology functions have been used in this study (Fig. 4):

1. Isotropic growth (growth rate is independent of α).
2. 'Square mineral'. The growth rate has a sharp minimum at 45° to the *c*-axis. In free growth this gives square grains with crystal faces at 45° to the *c*-axis.
3. 'Prismatic mineral'. The growth function has two minima, one at 30° and one at 90° to the *c*-axis, which gives a prismatic shape with crystal face normals at 30 and 90° to the *c*-axis.

The morphology function gives the growth rate for a unit time increment. Growth can be slowed or accelerated by the user by the choice of the duration of a time step.

2.2. Movement of nodes

At each time step, all active nodes are moved once to simulate a small increment of growth. The movement of nodes involves the following stages (Fig. 5):

1. The incremental growth displacement vector for each active segment (bound by one or two active nodes) is calculated with the morphology function. This vector is added to the mid-point of the segment, to obtain the new position ($\boldsymbol{p}$) of the node at the left end of the segment, but that node is not yet moved to its new position, which is temporarily stored in memory for each node (Fig. 5a).
2. Displacement of a triple junction node needs a special routine. Such a node lies on two grains (grains A and B in Fig. 5) which have one shared boundary segment at that node. Four growth displacement vectors are calculated as in step (1) (Fig. 5b). Addition of each of these displacement to the centres of the segments gives four new positions: $\boldsymbol{p}_{A1}$, $\boldsymbol{p}_{A2}$, $\boldsymbol{p}_{B1}$ and $\boldsymbol{p}_{B2}$, representing two new segments: $\boldsymbol{p}_{A1}$–$\boldsymbol{p}_{A2}$ and $\boldsymbol{p}_{B1}$–$\boldsymbol{p}_{B2}$. The intersection of these two new segments is taken as the new position of the triple junction node. This routine may seem overly complicated, but all it actually does is first assume that the two neighbouring grains grow outward into the fracture and over each other. As overlaps are impossible, the new triple node position is at the intersection of the displaced boundaries.
3. When all new positions are calculated, all nodes are moved to their new positions (Fig. 5c).
4. Maintenance and checks are performed at the end of each time step (Fig. 5d).

   A user-defined limited segment length range is maintained by adding double nodes when segments

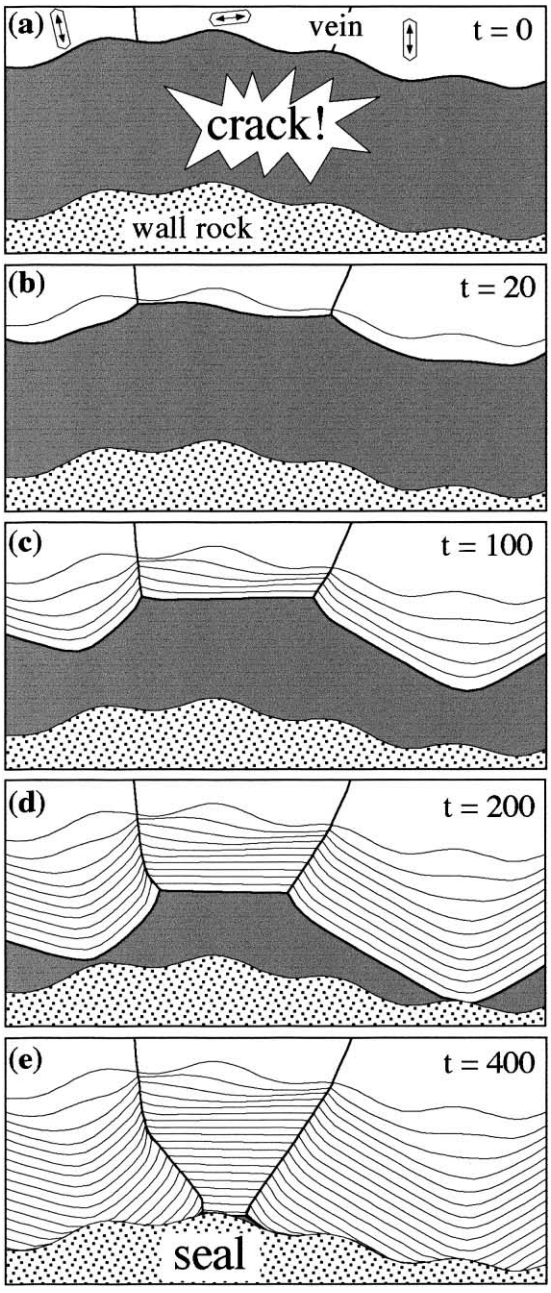

Fig. 6. Detail of one whole crack-seal increment in 400 time steps, from initial opening of the crack at (a) to full sealing at (e). Small prisms with double arrows represent the orientation of the *c*-axes of the 'prismatic mineral'. Overgrowth of crystals quickly changes the growth surface from the crack-shape to crystallographically controlled facets (b–d).

are too long or by removing nodes when segments become too short.

Node positions are checked for having reached the opposite side of the fracture, in which case they are locked until the next fracture opening event (Fig. 3b). When the growing tip of a grain becomes too narrow (less than one third of the maximum segment length), the two triple nodes at the tip are re-arranged to terminate the grain and make its two neighbouring grains neighbours of each other (Fig. 5e).

2.3. Input and output

The user can input a range of variables:

1. The number of time steps, their duration and crack opening history.
2. The growth morphology or growth-rate function.
3. The initial fracture shape and grain seeds array or the 'starting vein'. A starting vein with a wavy surface can be automatically generated by the program. The waviness is made by superposition of two sine and one cosine functions for which the user can set the wavelengths and amplitudes. The starting vein can also be made from a drawing or scanned image to resemble a natural case.

During run time, an image in PICT-file format is saved every user-defined number of time steps. Initial settings, run time statistics (such as number of actively growing grains) are recorded on the image, as well as a rose diagram of the *c*-axes orientation frequency distribution of actively growing grains. These statistics are also recorded in a TEXT-format log file that can be incorporated into any spreadsheet program. At any time the user can interrupt the program to save the current geometry for later continuation of the simulation.

3. Example of results

The accompanying paper by Hilgers et al. (2000), presents a first analysis of the role of different parameters on the crystal morphology of veins, using the model that is discussed here. Only a brief example of the application of the model is therefore given here. Fig. 6 shows a detailed simulation of one crack-seal event, using the 'prismatic mineral'. The growth surface has the shape of the crack immediately after opening of the crack. The shape of the surface quickly changes to one controlled by the crystallography of the growing crystals (Fig. 6b and c). The grains on the left and right have their fast growth direction approximately perpendicular to the fracture and these reach the opposite side of the fracture first. They also expand laterally, at the expense of the central grain.

Fig. 7 shows a range of results for the three different 'minerals' and different settings. The first row of images shows simulations of growth in to a wide fluid-filled space. Anisotropic growth leads to a faceted growth surface, as found in geodes for instance. A distinct crystallographic preferred orientation develops in the 'winner' grains. The other images in Fig. 7 show the effect that different fracture roughnesses have for the different 'minerals'. The smoothest surface gives very poor tracking of the curved

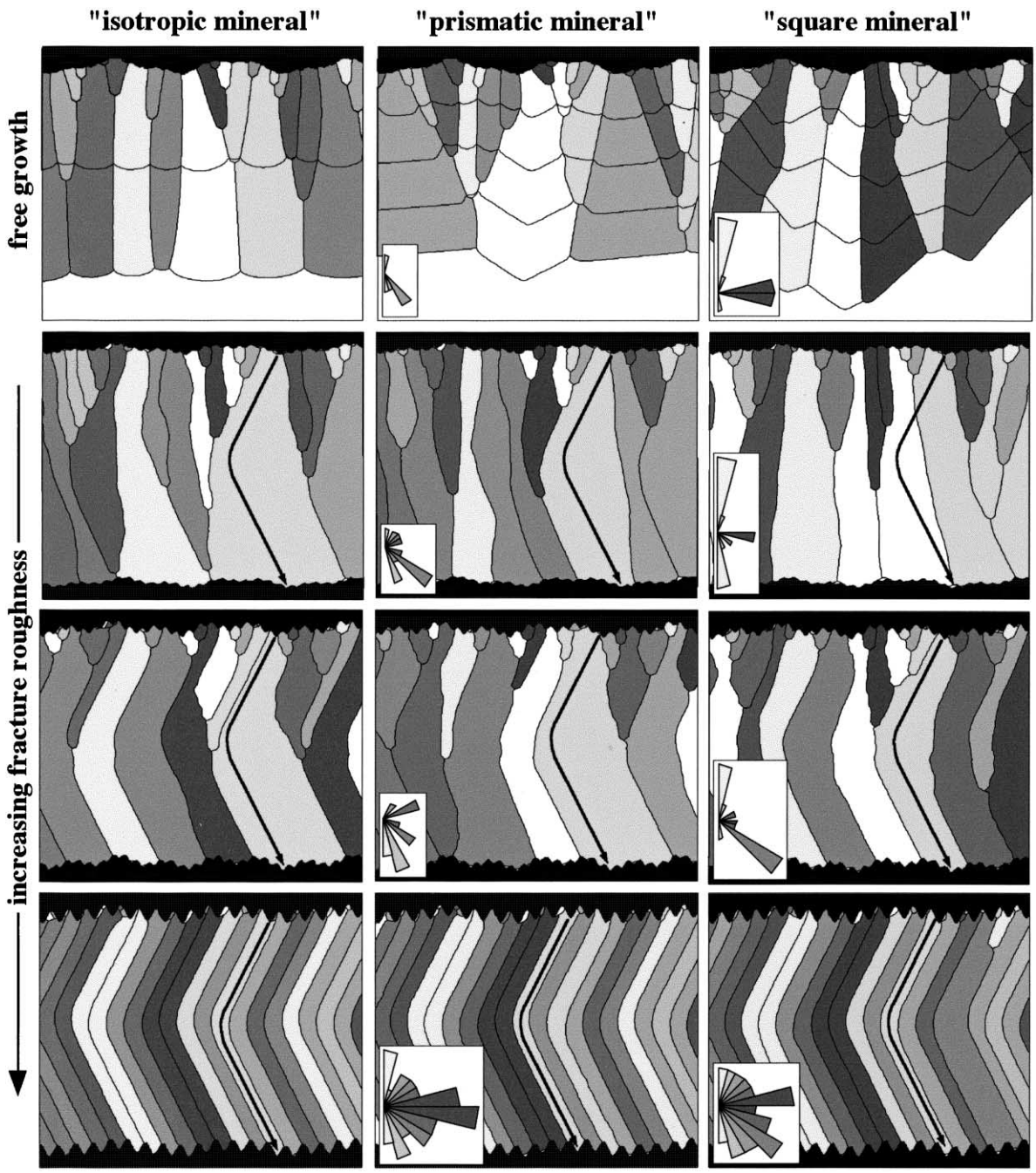

Fig. 7. Some examples of simulations with the numerical model. Identical simulations were done with the 'isotropic mineral' (left column), the 'prismatic mineral' (centre column) and the 'square mineral' (right column). First row shows free growth in a wide open crack. Lines show the vein surface in 200 time steps intervals. Other rows show crack-seal simulations with a curved opening trajectory (arrow) and increasing fracture roughness. The crack was opened 50 times, once every 100 time steps. Vertical crack width was 8 pixels and the maximum distance between nodes was 8 pixels. Rose diagrams to the right of images show the *c*-axis orientation distribution of surviving crystals. These diagrams represent more grains than shown, as only half of each whole 1000-pixel-wide model with 100 seed grains is shown here. See text for discussion.

opening trajectory, especially for the 'square mineral'. Although the 'prismatic mineral' shows very poor tracking, the maximum is parallel to the last opening direction. This suggests that the crystallographic preferred orientation in a vein may contain information about the opening trajectory, even if the vein crystals themselves do not track the opening trajectory. Medium fracture roughness produces better tracking, but still an elongate-blocky microstructure with significant growth competition and a crystallographic preferred orientation. Only the roughest surface in the

example gives a perfectly tracking fibrous microstructure, with the fibre width completely determined by the spacing between the ridges.

4. Limitations and possible future improvements

The major limitation of the model is that it is two-dimensional. It is tempting to directly compare images with thin sections, but the latter are two-dimensional sections through three-dimensional samples. Bearing this difference in mind, the program can give valuable insight in what happens in real three-dimensional veins.

As yet, the wall rock is treated as rigid and only moving down and to the left or right. There is no pivoting or deformation of the wall rock. It is therefore currently not possible to use the program to study what happens at a propagating vein tip. This is however not an intrinsic limitation of the program. Incorporating vein tip processes as well as complicated opening geometries in pressure fringes are the subject of current work.

The program essentially simulates what happens in one half of an antitaxial vein, where the fracture shape is dictated by the wall rock surface and can be assumed to remain close to constant. In syntaxial and ataxial or stretching veins (Ramsay and Huber, 1983; Passchier and Trouw, 1996), the fracture shape is not constant at all, but this cannot be modelled with the current program.

Relatively minor changes and additions are planned to make it possible to have more than one mineral in a vein and to have ongoing nucleation of crystals in the vein.

5. Conclusions

The program presented here provides a powerful tool for teaching and research to explore microstructural developments in elongate-blocky and fibrous veins. The effect of controlling parameters, such as fracture shape, opening trajectory and mineral growth morphology can be studied with it in a systematic way. First results are presented in part II of this paper (Hilgers et al., 2001).

The program (for Macintosh computers) can be obtained from the author via the WWW-address: http://www.uni-mainz.de/FB/Geo/Geologie/tecto

Acknowledgements

The author wishes to thank Mark Jessell for his help with the programming. Mark Jessell, Chris Hilgers, Daniel Köhn and Janos Urai are thanked for helpful discussions and their interest in application of the program. Win Means and Stephen Cox are thanked for their positive reviews. The author acknowledges past financial support from the Australian Research Council through a postdoctoral research fellowship and current support from Monash University through a Logan Research Fellowship.

References

Bons, P.D., Jessell, M.W., 1997. Experimental simulation of the formation of fibrous veins by localised dissolution-precipitation creep. Mineralogical Magazine 61, 53–63.

Cox, S.F., 1987. Antitaxial crack-seal vein microstructures and their relationship to displacement paths. Journal of Structural Geology 9, 779–787.

Cox, S.F., Etheridge, M.A., 1983. Crack-seal fibre growth mechanisms and their significance in the development of oriented layer silicate microstructures. Tectonophysics 92, 147–170.

Durney, D.W., Ramsay, J.G., 1973. Incremental strains measured by syntectonic crystal growth. In: de Jong, K.A., Scholten, R. (Eds.), Gravity and Tectonics. Wiley, New York, pp. 67–96.

Fisher, D.M., Brantley, S.L., 1992. Models of quartz overgrowth and vein formation: deformation and episodic fluid flow in an ancient subduction zone. Journal of Geophysical Research 97 (B13), 20,043–20,061.

Hilgers, C., Köhn, D., Bons, P.D., Urai, J.L., 2001. Development of crystal morphology during unitaxial growth in a progressively widening vein: II. Numerical simulations of the evolution of antitaxial fibrous veins. Journal of Structural Geology 23, 873–885.

Jessell, M.W., Willman, C.E., Gray, D.R., 1994. Bedding parallel veins and their relationship to folding. Journal of Structural Geology 16, 753–767.

Mügge, O., 1928. Über die Entstehung faseriger Minerale und ihrer Aggregationssformen. Neues Jahrbuch für Mineralogie, Geologie und Paläontologie 58A, 303–348.

Passchier, C.W., Trouw, R.A.J., 1996. Microtectonics. Springer, Berlin.

Passchier, C.W., Urai, J.L., 1988. Vorticity and strain analysis using Mohr diagrams. Journal of Structural Geology 10, 755–763.

Ramsay, J.G., 1980. The crack-seal mechanism of rock deformation. Nature 284, 135–139.

Ramsay, J.G., Huber, M., 1983. Strain Analysis. The Techniques of Modern Structural Geology, Vol. 1. Academic Press, London.

Spencer, S., 1991. The use of syntectonic fibres to determine strain estimates and deformation paths: An appraisal. Tectonophysics 194, 13–34.

Urai, J.L., Williams, P.F., van Roermund, H.L.M., 1991. Kinematics of crystal growth in syntectonic fibrous veins. Journal of Structural Geology 13, 823–836.

Williams, P.F., Urai, J.L., 1989. Curved vein fibres: an alternative explanation. Tectonophysics 158, 311–333.